PHYSICAL REVIEW E **96**, 040701(R) (2017)

Visual evaluation of surface anchoring strength by electrohydrodynamic convection of a nematic liquid crystal

Gyu Jin Choi,[1] Jae Min Song,[1] Chul Gyu Jhun,[2] Jong-Hoon Huh,[3,*] and Jin Seog Gwag[1,*]

[1]*Department of Physics, Yeungnam University, 280 Daehak-Ro, Gyeongsan 38541, Republic of Korea*

[2]*School of Display Engineering, Hoseo University, Asan-shi, Chungnam 31499, Republic of Korea*

[3]*Department of Mechanical Information Science and Technology, Faculty of Computer Science and Systems Engineering, Kyushu Institute of Technology, Iizuka, Fukuoka 820-8502, Japan*

(Received 4 August 2017; published 30 October 2017)

Visual evaluation of the surface anchoring energies in a nematic liquid crystal (LC) cell is characterized by the direction of the convection roll pattern that appears in the low-frequency conduction regime. The convection roll pattern in a twisted nematic LC (TNLC) cell is oriented perpendicular to the midplane LC director dominating the direction of convection flow, and its direction is determined by the relative surface anchoring energy between two surface boundaries. Thus the direction of the roll pattern generated at the TNLC cell with asymmetric LC alignment layers can provide information on the surface anchoring energies at the two boundaries. We demonstrate a method for determining the two anchoring energies through a measured midplane LC director applied to the Ericksen-Leslie equation.

DOI: 10.1103/PhysRevE.96.040701

The surface and bulk properties of liquid crystal (LC) cells with anchoring boundaries have been studied extensively owing to their significance in both high-technology LC applications [1–3] including recent biotrepy and basic science [4–10]. Furthermore, the surface anchoring strength of LCs is a crucial factor that seriously affects the electro-optic characteristics of LC devices [11–13]. Thus several techniques for measuring the surface anchoring strength have been tried using optical methods. The almost fundamental concept of such techniques is to find the surface LC deviation angle with respect to the easy axes produced by rubbing or light exposure treatment based on the competition between the bulk elastic energy F_b and the surface anchoring energy F_s [14–23]. In more detail, for a twisted LC state, the total free energy per unit area, F_t, from the torque balance equation and continuum theory, can be expressed as the sum of F_b and F_s, which are written as $F_b = (k_{22}/2d)(\phi - 2\pi d/p)^2$ and $F_s = 1/2A\sin^2\Delta\phi$, where d is the cell thickness, k_{22} is the twist elastic constant, ϕ is the twist angle, p is the chiral pitch of the LC, A is the azimuthal anchoring energy of the LC, and $\Delta\phi$ is the azimuthally deviated angle of the LC surface from the easy axis. By minimizing F_t, A can be obtained as follows:

$$A = \frac{2k_{22}}{\sin(2\Delta\phi)}\left(\frac{\phi}{d} - \frac{2\pi}{p}\right). \tag{1}$$

In Eq. (1), if $\Delta\phi$ is determined, then A can be obtained. Optical methods have been used to determine $\Delta\phi$. The transmission T in a twisted nematic LC (TNLC) is given by

$$T = \left[\cos\beta\cos(\varphi - \delta + \alpha - 2\Delta\phi) + \frac{\varphi - 2\Delta\phi}{\beta} \times \sin\beta\sin(\varphi - \delta + \alpha - 2\Delta\phi)\right]^2 + \frac{\eta^2}{\beta^2}\sin^2\beta\cos^2(\varphi - \delta - \alpha), \tag{2}$$

where η and β are defined as $\eta = \pi d\Delta n/\lambda$ and $\beta = \sqrt{\eta^2 + (\varphi - 2\Delta\phi)^2}$ with φ representing the angle between the two easy axes (rubbing directions) of the top and bottom substrates; α and δ are the angles of the input and output polarizers, respectively, with respect to the easy axis; and Δn and λ are, respectively, the birefringence of the LC used and the wavelength of light. In Eq. (2), we can obtain $\Delta\phi$ by satisfying the value of β at a given λ whose T becomes minimum or maximum. However, when $\Delta\phi$ is a very small angle, meaning a strong anchoring boundary, this technique may give rise to large measurement error because it is not easy to distinguish optically between φ and $\varphi + \Delta\phi$. Furthermore, the precondition with which these methods can be established is that the deviation angle of the LC, $\Delta\phi_t$, in the top substrate must be the same with that, $\Delta\phi_b$, in the bottom substrate. In other words, they cannot be applied to asymmetric anchoring boundaries that have different anchoring strengths at the top and bottom surfaces.

Electrohydrodynamic convection (EHC) of an LC occurs when a low-frequency electric field is applied across an aligned nematic LC layer of an appropriate thickness (typically 10–100 μm) with sufficient ionic conductivity [24–27]. EHC is caused by hydrodynamic instability resulting from the fast movement of local charges by the Coulomb force [28–37]. Then various patterns are formed by EHC under properly applied alternating electric fields. The Williams domain, which appears in the low-frequency conduction regime, is the most representative pattern and the basic pattern of EHC resulting from the Carr-Helfrich instability [27]. EHC in a TNLC has been also investigated, and one important result is that the Williams rolls are oriented perpendicular to the midplane director of the undisturbed layer [38,39]. Therefore, we can ascertain the LC direction of the midplane by directly observing the direction of the convection rolls in EHC of a TNLC through a microscopic image. In symmetric anchoring boundaries that have the same anchoring strengths at the top and bottom surfaces, the midplane LC director in a 90°-TNLC cell is always 45°; $\varphi = 90^\circ \rightarrow \phi_m = \phi(z = d/2) = 45^\circ$. However, in asymmetric anchoring boundaries,

*huh@mse.kyutech.ac.jp; sweat3000@ynu.ac.kr

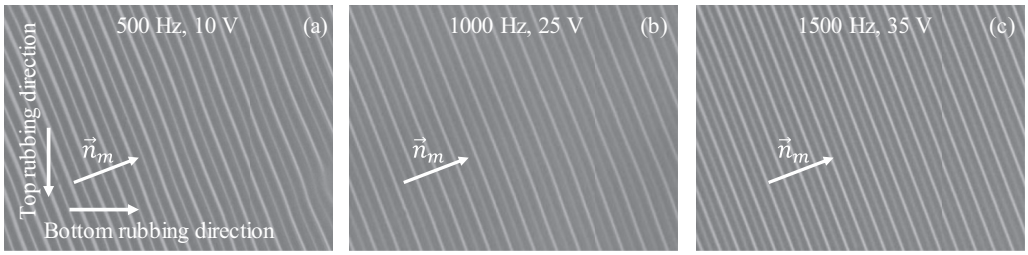

FIG. 1. Microscopic images showing typical Williams convection roll patterns taken from an asymmetric asymmetric 90°-TNLC cell of 10 μm that has strong surface anchoring at the bottom boundary (PI) and weak surface anchoring at the top boundary (PVA), under voltage and frequency of (a) 10 V and 500 Hz, (b) 25 V and 1000 Hz, and (c) 35 V and 1500 Hz. The roll direction is not changed even under a strong electric field.

the director points toward the stronger anchoring boundary, deviating from 45°. Eventually, the LC direction will be changed depending on the difference of the two anchoring strengths.

Here, we will introduce a simple method for determining the LC anchoring strengths on two surfaces by directly finding the LC direction in the midplane through the roll direction produced by using a TNLC cell with asymmetric anchoring boundaries.

The total free energy, in terms of $\vec{n}$, is [40]

$$F = \frac{1}{2}\int_0^d \Big[k_{11}(\nabla\cdot\vec{n})^2 + \frac{1}{2}k_{22}(\vec{n}\cdot\nabla\times\vec{n})^2 + \frac{1}{2}k_{33}(\vec{n}\times\nabla\times\vec{n})^2 - \frac{1}{2}\varepsilon_0\Delta\varepsilon(\vec{n}\cdot\vec{E})^2\Big]dz + \frac{1}{2}A_t\sin^2(\Delta\phi_t) + \frac{1}{2}A_b\sin^2(\Delta\phi_b) + \frac{1}{2}W_t\sin^2(\Delta\theta_t) + \frac{1}{2}W_b\sin^2(\Delta\theta_b), \quad (3)$$

where k_{11},k_{22}, and k_{33} pertain to splay, twist, and band deformations, respectively, as elastic constants; $\Delta\theta_t$ and $\Delta\theta_b$ are the zenithally deviated angles of the surface LC from the easy axis at the top and bottom surfaces, respectively; A_t and A_b are the azimuthal anchoring energies at the top and bottom surfaces, respectively; W_t and W_b are the polar anchoring energies at the top and bottom surfaces, respectively; $\vec{n}(n_x,n_y,n_z)$ is the LC director; and $\Delta\varepsilon$ is the dielectric anisotropy. For the dynamics of the LC directors, the Ericksen-Leslie equation [40,41] is used:

$$\gamma_1\frac{dn_i}{dt} = \left(\frac{\partial F}{\partial n_{i,j}}\right) - \frac{\partial F}{\partial n_i} - \gamma_1 B_{i,j}n_j - \frac{1}{2}\gamma_2 G_{i,j}n_j (i,j = x,y,z), \quad (4)$$

where γ_1 and γ_2 are the rotational viscosity and torsion coefficient, respectively, and $B_{i,j}$ and $G_{i,j}$ are the antisymmetric and symmetric parts of the gradient velocity, respectively, written as $1/2(v_{j,i} - v_{i,j})$ and $1/2(v_{j,i} + v_{i,j})$ via the Navier-Stokes equation [42] including fluid density and Leslie coefficients. When the Leslie coefficients are not known, it is not easy to solve Eq. (4). Nevertheless, Fig. 1 gives us a clue to the solution of the problem. It shows microscopic images of typical Williams convection roll patterns according to the electric field taken from an asymmetric LC cell that has strong surface anchoring at the bottom boundary and weak surface anchoring at the top boundary. As shown in Fig. 1, the roll direction is not changed even under a strong electric field. This means that any variation of the EHC director field in the bulk driven by the electric field does not occur or is not large enough to change the surface director. This result may be due to the use of an LC [*p*-methoxybenzylidene-*p*′-*n*-butylaniline (MBBA)]

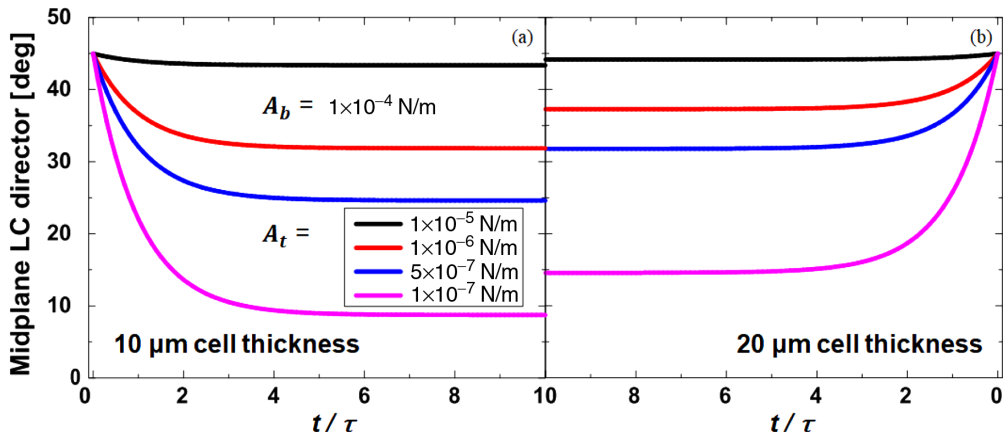

FIG. 2. Simulated dynamics of the director at the midplane in 90°-TNLC cells of thicknesses of 10 (a) and 20 μm (b) under an electric field of 1.5 V/μm when $A_b = 10^{-4}$ N/m, and $A_t = 10^{-5}$,10^{-6},5×10^{-7}, and 10^{-7} N/m, showing clearly the thickness dependence of the director. The thicker the thickness is, the smaller the angle deviated from 45° is, as expected.

with negative dielectric anisotropy and a homogeneous LC alignment [polyimide (PI); SE-3140 provided by Nissan Chemical] for the bottom boundary and counterhomogeneous LC alignment [polyvinyl alcohol (PVA)] for the top boundary rubbed by velvet. Negative LCs aligned in plane are nearly unmoved by the vertical electric field. Furthermore, as seen in Fig. 1, the orientation of the midplane director perpendicular to the rolls was not changed even by director instability resulting from fast-flow convection by a strong field. Thus the flow-related terms in Eq. (4) can be ignored in investigating the change of the LC direction at the midplane ($z = d/2$) according to the two surface anchoring energies. $\partial\phi/\partial z$ is constant; i.e., $\partial\phi/\partial z = (\pi/2 - \Delta\phi_t - \Delta\phi_b)/d$ and $\partial\theta/\partial z \approx 0$. The polar anchoring strength W does not have a significant impact on the azimuthal anchoring strength A because of the orthogonality of the two forces. Here $W = 7A$ was used because, in general, W is within $5A$–$10A$ [23]. The k_{11},k_{22},k_{33}, and $\Delta\varepsilon$ of MBBA are 6.66 pN, 4.2 pN, 8.61 pN, and 0.53, respectively [38]. In the absence of flow, we calculated Eq. (4) approximately to obtain the director at the midplane for the case of $A_t \neq A_b$. Figure 2 shows the dynamics of the director at the midplane in a 90°-TNLC cell of thicknesses of 10 and 20 μm under an electric field of 1.5 V/μm when $A_b = 10^{-4}$ N/m, and $A_t = 10^{-5}$,10^{-6},5×10^{-7}, and 10^{-7} N/m. As expected, the director shifts azimuthally to the stronger anchoring surface from $\phi_m = 45^\circ$ and, the larger A_b/A_t is, the more it shifts toward it. The director relaxation at the midplane when $\phi_m(0) = \pi/4$ and $\phi_m(\infty) = \phi_f$ may be expressed as $\phi_m(t) = (\pi/4 - \phi_f)e^{-t/\tau} + \phi_f$. Thus ϕ_f determined by the relative anchoring strength of the top and bottom boundaries becomes the azimuthal angle of the LC director $\vec{n_m}$ of the midplane in the equilibrium state and can be easily measured experimentally by the direction of the convection roll pattern, which is perpendicular to the director of the midplane.

Figures 3(a) and 3(b) show microscopic images of the EHC taken for a 90°-TNLC cell of 10 μm cell thickness when PI was used for the bottom surface and PVA and SiO_2 were used for the top surfaces as homogeneous LC alignment layers. ϕ_f was 21.5° for PVA/PI and 19.0° for SiO_2/PI, as shown in Figs. 3(a) and 3(b), respectively. When one of the two anchoring energies is known, the remaining one can be determined easily by measuring ϕ_f. Figure 3(c) is a graph showing A_t according to ϕ_f, obtained from Eq. (4), when A_b is 3.48×10^{-5} N/m, the azimuthal anchoring energy of SE-3140 after rubbing [18]. Then we can determine easily the anchoring energies of PVA and SiO_2. As indicated in Fig. 3(c), 21.5° and 19.0° for ϕ_f correspond to the azimuthal anchoring energies of 3.72×10^{-7} N/m for PVA and 2.95×10^{-7} N/m for SiO_2, respectively. These values are somewhat different from the previous results, but not significantly [19,43,44].

If neither of these values is known, we need a wedge cell to measure ϕ_f at two different cell thicknesses. It is very natural that, for the same twist, the larger the cell thickness is, the less effect the elastic energy has on the bulk. Therefore, when the cell thickness changes, the deviation angle at the surface is changed and then ϕ_f is also changed necessarily, as shown in Fig. 2. Figure 4 shows microscopic images of EHC taken for 90°-TNLC cells of 20 and 40 μm cell thicknesses. In the case

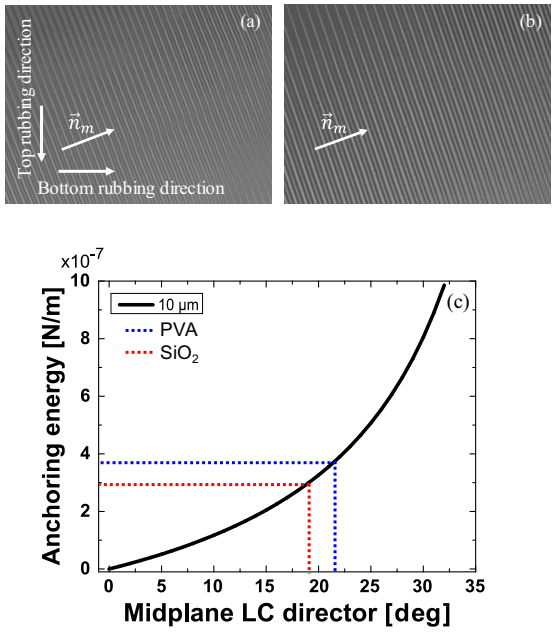

FIG. 3. Microscopic images of the EHC taken for a 90°-TNLC cell of 10 μm cell thickness when PI was used for the bottom surface and PVA (a) and SiO_2 (b) were used for the top surfaces as homogeneous LC alignment layers. ϕ_f was 21.5° for the combination of PVA/PI and 19.0° for the combination of SiO_2/PI. When the azimuthal anchoring energy of PI, A_b, is known as 3.48×10^{-5} N/m, the anchoring energies of PVA and SiO_2 corresponding to the ϕ_f are 3.72×10^{-7} and 3×10^{-7} N/m, respectively, as shown in (c).

of 20 μm cell thickness, ϕ_f was 29.0° for PVA/PI and 27.0° for SiO_2/PI, as shown in Figs. 4(a) and 4(b), respectively. In contrast, for 40 μm cell thickness, ϕ_f was 35.0° for PVA/PI and 34.0° for SiO_2/PI, as shown in Figs. 4(c) and 4(d), respectively. Figure 4(e) shows a graph of A_t with A_b, obtained from Eq. (4) when ϕ_f is 29.0° and 35.0° for PVA/PI for 20 and 40 μm cell thicknesses, respectively. We can also simply determine the two anchoring energies by the cross pointing of the two curved lines shown in Fig. 4(e), which indicates the numerical solution simultaneously satisfying the two results measured from each cell thickness. As a result, we obtained the two anchoring energies: 3.81×10^{-5} N/m for PI and 3.68×10^{-7} N/m for PVA. Even if there are slight differences, these values match well with the previous values. In the same manner, from Fig. 4(f), we determined the azimuthal anchoring energies of the PI and SiO_2 to be 3.86×10^{-5} and 3.14×10^{-7} N/m. The slight difference from the result of the anchoring energy of PI obtained in Fig. 4(e) is due to the slight difference of cell thickness between two LC cells. Consequently, we conclude that this method is very useful in terms of ease, simplicity, and accuracy for determining the surface anchoring energy of the LC alignment layer.

We can also ignore the electric field term in Eq. (4) because the role of the vertical electric field on the horizontally aligned negative LC is insignificant for deforming LCs. Then Eq. (4) can be reduced to static properties. Here, for simplicity, we use the one-elastic-constant approximation ($k_{11} = k_{22} = k_{33}$) and assume that W_t and W_b are very strong anchoring energies. In this case having pure twist deformation, k_{22} is representative of k. Therefore, the total free energy of the TNLC for small

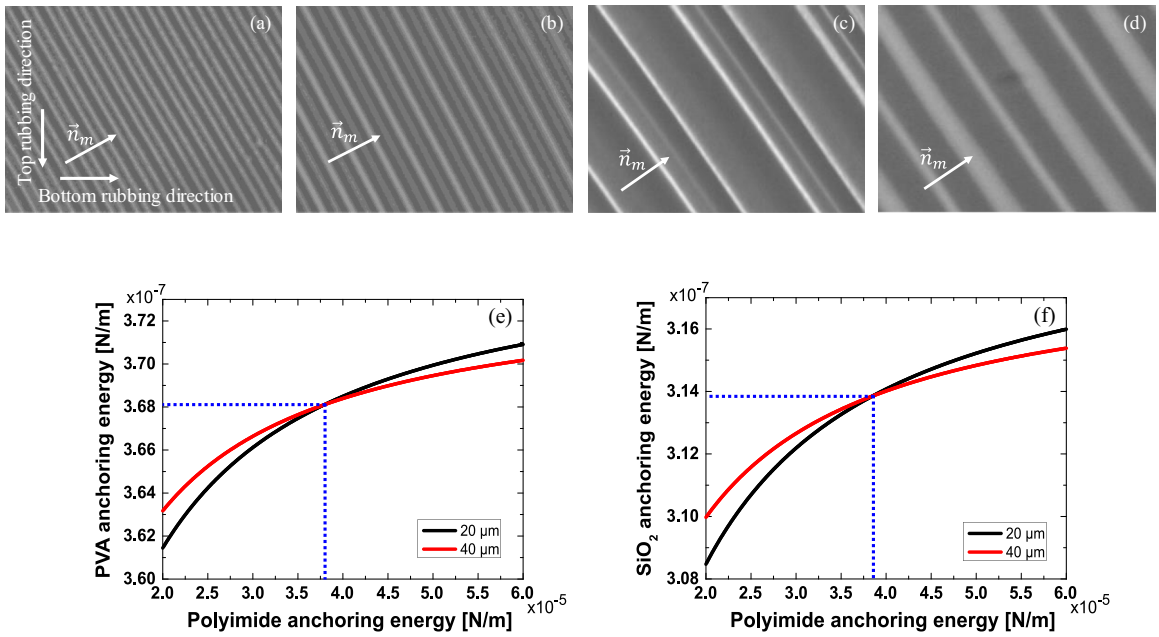

FIG. 4. Microscopic images of EHC taken for 90°-TNLC cells, with PVA/PI (a) and SiO_2/PI (b) of 20 μm cell thickness and with PVA/PI (c) and SiO_2/PI (d) of 40 μm cell thickness. (e,f) show plotting of A_t with A_b, obtained from Eq. (4) for PVA/PI and SiO_2/PI, respectively, when ϕ_f is given as 29.0°, 27.0°, 35.0°, and 34.0° by (a–d), respectively. The unknown two anchoring energies are determined by the cross pointing of the two curved lines.

$\Delta\phi$ can be given by

$$F = \frac{1}{2}k_{22}\int_0^d \left(\frac{d\phi}{dz}\right)^2 dz + \frac{1}{2}A_t(\Delta\phi_t)^2 + \frac{1}{2}A_b(\Delta\phi_b)^2. \quad (5)$$

Because infinitesimal variation of the free energy in steady state is zero, by minimizing Eq. (5), we obtain one stable distribution of the director and two boundary conditions as $d^2\phi/dz^2 = 0$, $-k_{22}d\phi/dz + A_b\phi = 0$ at $z = 0$, and $k_{22}d\phi/dz - A_t(\varphi - \phi) = 0$ at $z = d$, where φ is the angle between the easy axes and 90° in our case. By taking into account the three conditions, we obtain finally the twist angle at 0 to d for continuous positions of z in the LC cell as follows:

$$\phi = \frac{A_t\varphi}{k_{22}(1 + A_t/A_b) + A_t d}(z + k_{22}/A_b). \quad (6)$$

By directly measuring the directors at the midplane, $z{=}d/2$, through the convection roll patterns, we can determine the surface anchoring energies. Equation (6) is an approximate algebraic solution of the static state and, for smaller deviation of $\Delta\phi$ ($<10°$), agrees well with the numerically estimated data from Eq. (4) indicating dynamics.

We have examined a method to determine the surface anchoring energies in a TNLC cell with asymmetric alignment layers by using the Williams convection roll pattern of the conduction regime. Unlike the conventional method, in which the wavelength or rotation angle of minimum or maximum light intensities is determined through cell rotation or polarizer rotation, this method enables visual evaluation through a microscopic image for the direction of the roll pattern. Thus, in terms of ease, simplicity, and accuracy, we believe that our method is largely superior to the conventional one.

We thank Hiroshi Yokoyama for useful discussions. This work was supported through the Basic Science Research Program through the National Research Foundation of Korea (NRF) funded by the Ministry of Science, ICT, and Future Planning (Grant No. 2016R1D1A3B03932396).

[1] S. J. Woltman, G. D. Jay, and G. P. Crawford, Nat. Mater. **6**, 929 (2007).
[2] J. H. Kim, M. Yoneya, and H. Yokoyama, Nature **420**, 159 (2002).
[3] G. J. Choi, Q. V. Le, K. S. Choi, K. C. Kwon, H. W. Jang, J. S. Gwag, and S. Y. Kim, Adv. Matter. **29**, 1702598 (2017).
[4] D. W. Berreman, Phys. Rev. Lett. **28**, 1683 (1972).
[5] S. Faetti and P. Marianelli, Phys. Rev. E **72**, 051708 (2005).
[6] J. S. Gwag, J. Fukuda, M. Yoneya, and H. Yokoyama, Appl. Phys. Lett. **91**, 073504 (2007).
[7] J. S. Gwag, J. H. Kwon, M. Oh-e, J. Niitsuma, M. Yoneya, and H. Yokoyama, Appl. Phys. Lett. **95**, 103101 (2009).
[8] H. Yokoyama and H. A. van Sprang, J. Appl. Phys. **57**, 4520 (1985).
[9] T. Araki, M. Buscaglia, T. Bellini, and H. Tanaka, Nat. Mater. **10**, 303 (2011).
[10] J. I. Fukuda, M. Yoneya, and H. Yokoyama, Phys. Rev. Lett. **98**, 187803 (2007).
[11] G. P. Bryan-Brown, E. L. Wood, and I. C. Sage, Nature **399**, 338 (1999).

[12] J. H. Kim, W. S. Kang, H. S. Choi, K. Park, J. H. Lee, S. Yoon, S. Yoon, G.-D. Lee, and S. H. Lee, J. Phys. D: Appl. Phys. **48**, 465506 (2015).
[13] L. Weng, P.-C. Liao, C.-C. Lin, T.-L. Ting, W.-H. Hsu, J.-J. Su, and L.-C. Chien, AIP Adv. **5**, 097218 (2015).
[14] J. S. Gwag, S. J. Kim, J. G. You, J. Y. Lee, J. C. Kim, and T.-H. Yoon, Opt. Lett. **30**, 1387 (2005).
[15] M. Jiang, Z. Wang, R. Sun, K. Ma, R. Ma, and X. Huang, Jpn. J. Appl. Phys. **33**, L1242 (1994).
[16] S. Okutani, M. Kimura, H. Toriumi, K. Akao, T. Tadokoro, and T. Akahane, Jpn. J. Appl. Phys. **40**, 244 (2001).
[17] Y. Zhou, Z. He, and S. Sato, Jpn. J. Appl. Phys. **36**, 2760 (1997).
[18] J. S. Gwag, J. Yi, and J. H. Kwon, Opt. Lett. **35**, 456 (2010).
[19] V. P. Vorflusev, H.-S. Kitzerow, and V. G. Chigrinov, Jpn. J. Appl. Phys. **34**, L1137 (1995).
[20] Y. Saitoh and A. Lien, Jpn. J. Appl. Phys. **39**, 1743 (2000).
[21] T. Akahane, H. Kaneko, and M. Kimura, Jpn. J. Appl. Phys. **35**, 4434 (1996).
[22] Y. Iimura, N. Kobayashi, and S. Kobayashi, Jpn. J. Appl. Phys. **33**, L434 (1994).
[23] Y. Choi, H. Yokoyama, and J. S. Gwag, Opt. Express **21**, 12135 (2013).
[24] R. Williams, J. Chem. Phys. **39**, 384 (1963).
[25] E. F. Carr, Mol. Cryst. Liq. Cryst. **7**, 253 (1969).
[26] L. Kramer and W. Pesch, Annu. Rev. Fluid Mech. **27**, 515 (1995).
[27] S. Kai and W. Zimmermann, Prog. Theor. Phys. Suppl. **99**, 458 (1989).
[28] W. Helfrich, J. Chem. Phys. **51**, 4092 (1969).
[29] M. C. Cross and P. C. Hohenberg, Rev. Mod. Phys. **65**, 851 (1993).
[30] T. Toth-Katona and J. T. Gleeson, Phys. Rev. E **69**, 016302 (2004).
[31] J. T. Gleeson, Phys. Rev. E **63**, 026306 (2001).
[32] P. Coullet, L. Gil, and J. Lega, Phys. Rev. Lett. **62**, 1619 (1989).
[33] G. Goren, I. Procaccia, S. Rasenat, and V. Steinberg, Phys. Rev. Lett. **63**, 1237 (1989).
[34] T. Toth-Katona, N. Eber, and A. Buka, Phys. Rev. E **83**, 061704 (2011).
[35] J.-H. Huh, Phys. Rev. E **92**, 062504 (2015).
[36] J.-H. Huh, Y. Hidaka, A. G. Rossberg, and S. Kai, Phys. Rev. E **61**, 2769 (2000).
[37] J.-H. Huh, Y. Yusuf, Y. Hidaka, and S. Kai, Phys. Rev. E **66**, 031705 (2002).
[38] A. Hertrich, A. Krekhov, and O. Scaldin, J. Phys. II **4**, 239 (1994).
[39] V. A. Deleva, P. Toth, and A. P. Krekhov, Mol. Cryst. Liq. Cryst. **351**, 179 (2000).
[40] P. G. de Gennes and J. Prost, *The Physics of Liquid Crystals* (Clarendon Press, Oxford, 1993).
[41] F. M. Leslie, Adv. Liq. Cryst. **4**, 1 (1979).
[42] D. J. Tritton, *Physical Fluid Dynamics* (Clarendon Press, Oxford, 1988).
[43] M. Behdani, S. H. Keshmiri, S. Soria, M. A. Bader, J. Ihlenmann, G. Marowsky, and T. Rasing, Appl. Phys. Lett. **82**, 2553 (2003).
[44] S. Faetti, M. Nobili, and A. Schirone, Liq. Cryst. **10**, 95 (1991).